JOURNAL OF Evolutionary Biology

doi: 10.1111/jeb.12108

Ecomorphology of the African felid ensemble: The role of the skull and postcranium in determining species segregation and assembling history

M. M. MORALES* & N. P. GIANNINI*†

*Consejo Nacional de Investigaciones Científicas y Técnicas, Facultad de Ciencias Naturales e Instituto Miguel Lillo, San Miguel de Tucumán, Tucumán, Argentina
†Department of Mammalogy, American Museum of Natural History, New York, USA

Keywords:

Africa;
cranium;
ecomorphology;
ensemble;
Felidae;
postcranium;
species segregation.

Abstract

Morphology of extant felids is regarded as highly conservative. Most previous studies have focussed on skull morphology, so a vacuum exists about morphofunctional variation in postcranium and its role in structuring ensembles of felids in different continents. The African felid ensemble is particularly rich in ecologically specialized felids. We studied the ecomorphology of this ensemble using 31 cranial and 93 postcranial morphometric variables measured in 49 specimens of all 10 African species. We took a multivariate approach controlling for phylogeny, with and without body size correction. Postcranial and skull + postcranial analyses (but not skull-only analyses) allowed for a complete segregation of species in morphospace. Morphofunctional factors segregating species included body size, bite force, zeugopodial lengths and osteological features related to parasagittal leg movement. A general gradient of bodily proportions was recovered: lightly built, long-legged felids with small heads and weak bite forces vs. the opposite. Three loose groups were recognized: small terrestrial felids, mid-to-large sized scansorial felids and specialized *Acinonyx jubatus* and *Leptailurus serval*. As predicted from a previous study, the assembling of the African felid ensemble during the Plio-Pleistocene occurred by the arrival of distinct felid lineages that occupied then vacant areas of morphospace, later diversifying in the continent.

Introduction

Extant felids (Mammalia: Carnivora) are remarkably homogeneous morphologically (e.g. Kitchener, 1991; Christiansen, 2008; Sicuro & Oliveira, 2010; Sicuro, 2011). As typical hyper-carnivorous predators, these species share anatomical adaptations for a killing bite including a short rostrum, strong zygomatic arches, and canines and carnassials that are well developed at the expense of other dental elements being greatly reduced (Ewer, 1998). The crown-clade of extant felids originated in Asia c. 11 Myr ago (Johnson *et al.*, 2006). Today, felids are distributed in four major landmasses – North and South America, Eurasia and Africa, plus a number of islands of various sizes nearby those continents. Africa is home to a rich felid ensemble. Felids first entered Africa about 20 Myr (Werdelin, 2012) and at present, 10 species representing three separate felid lineages inhabit the continent (Wozencraft, 2005). These lineages arrived separately and radiated in the continent (Werdelin & Lewis, 2005; Johnson *et al.*, 2006; Werdelin *et al.*, 2010) giving rise to species with many interesting ecological or ecomorphological features. The combined presence of those species makes the African ensemble particularly interesting for the study of morphological structure. Of a small number of extant felids that exhibit some degree of sociality, the lion [*Panthera leo* (Linnaeus, 1758)] is the only species with a typical gregarious way of life, forming prides that are generally composed of 6 to 15 individuals (Haas *et al.*, 2005; Ranta & Kaitala, 2005; Fryxell *et al.*,

Correspondence: Miriam M. Morales, Consejo Nacional de Investigaciones Científicas y Técnicas, Facultad de Ciencias Naturales e Instituto Miguel Lillo, Miguel Lillo 205, San Miguel de Tucumán, Tucumán, CP 4000, Argentina.
Tel.: 54 0381 4239456;
e-mail: moralesmiriamm@gmail.com

2007). This large species retains forest felid proportions on its legs despite occurring in open habitats (Gonyea, 1976). The cheetah [*Acinonyx jubatus* (Schreber, 1775)] is more cursorial and faster than all other felids, reaching speeds of 29 ms^{-1} (Sharp, 1997). Because of this ability, skeletal morphology, myology and performance of this species was intensively studied (e.g. Hildebrand, 1959, 1961; Hildebrand & Hurley, 1985; Alexander, 1993; Sharp, 1997; Hudson *et al*., 2011a,b). Many cursorial adaptations were already found and described for this species, such as long legs, more parasagitally restricted movements and long lumbar space (Hildebrand, 1959, 1961; Gonyea, 1976; Alexander, 1993). The serval [*Leptailurus serval* (Schreber, 1776)] is a mid-sized felid specialized in small-mammal hunting. This felid stands with its long legs in tall grass, and uses its big ears to locate small rodents by sound; then it jumps with its four feet, falling vertically on its prey (Geertsema, 1985). *C. caracal* and *F. chaus* are known to have longer hind limbs in relation to forelimbs and this morphology was associated to their ability to hunt birds catching them as they take off by jumping high to hold them in mid-air (Skinner, 1979; Tyabji, 1990; Sunquist & Sunquist, 2002). *Felis margarita* Loche, 1858 and *Felis nigripes* Burchell, 1824 are the smallest species of the ensemble; both are arid-land specialists, although *F. nigripes* seems not able to live in extensive desert dune areas as *F. margarita* (Skinner & Smithers, 1990; Huang *et al*., 2002). *F. nigripes* also exhibits a slight digging ability (Sunquist & Sunquist, 2002). It is remarkable that despite the diversity of felids in Africa no truly arboreal species is found in the continent, and just one species, *Profelis aurata* of the caracal lineage, is a wet-forest specialist (Sunquist & Sunquist, 2009). This may be a response to two factors, prior presence of arboreal viverrids (Werdelin & Peigné, 2010) and a relatively scarce forest cover across the continent (Archibold, 1995).

Here, we focus on the morphofunctional structure of the African felid ensemble on the basis of skull and postcranial osteological variation, separately and in combination. Much of the attention devoted to felid morphometrics has been directed to describe skull morphology and function, at the level of assemblages or the entire family (Werdelin, 1983; Kiltie, 1984, 1988; Dayan *et al*., 1990; Christiansen, 2008; Meachen-Samuels & Van Valkenburgh, 2009a; Morales & Giannini, 2010; Sicuro & Oliveira, 2010; Sicuro, 2011). However, remarkable inter-specific variation exists in postcranial morphology. Felids are considered cursorial predators with certain specializations towards a jumping and sprinting way of life (Gonyea, 1976; Spoor & Badoux, 1988; Schmieder, 2000). Some postcranial characters such as limb-bone ratios have been found to be informative about habits and habitat preference of species (Gonyea, 1978; Werdelin & Lewis, 2005; Meachen-Samuels & Van Valkenburgh, 2009b). A few studies have characterized limb osteology and myology from a functional perspective; however, to our knowledge, these studies have been focussed on single species, such as *A. jubatus* (e.g. Hudson *et al*., 2011a,b). In addition, other studies on felid ensembles considered ecological parameters, for example, activity patterns and trophic and spatial segregation among sympatric species (e.g. Emmons, 1987; Konecny, 1989; Chinchilla, 1997). Clearly, a vacuum exists regarding the expression of morphometric variation in the postcranium of felids as a group, and how this variation interacts with that of the skull.

We begin exploring this theme by introducing a large morphometric database (93 variables) of functional morphology of the postcranium, measured in members of the African felid ensemble. We show here that postcranial variables are as important as, or more important than, cranial variables in terms of the inter-specific morphofunctional patterns they reveal at the ensemble level. We take into account the phylogenetic structuring of the morphological information and use the sequence of lineage origination and fossil record to understand the temporal assembling of the African felid ensemble. With this frame, our goal was to test predictions derived from a previous study on the South American ensemble (Morales & Giannini, 2010); specifically, that after their arrival into Africa, species segregate in morphospace and so presumably in function, and that those species that do overlap in morphospace further differ in ecological or behavioural attributes (Morales & Giannini, 2010; see Hutchinson, 1957 for a theoretical base). Our results shed light on the organization of this ensemble and about carnivoran coexistence within a group of antagonistic species.

Materials and methods

Specimens and variables

We examined a total of 49 specimens representing all 10 African felid species stored in the following institutions: American Museum of Natural History (AMNH), New York, the United States; Field Museum of Natural History (FMNH), Chicago, the United States; National Museum of Natural History (USNM), Washington D.C., the United States; Museo Argentino de Ciencias Naturales 'Bernardino Rivadavia' (MACN), Buenos Aires, Argentina. One such species, the jungle cat (*Felis chaus* Schreber, 1777), was excluded from the main analyses given its marginal distribution on the continent, but results including specimens of *F. chaus* are shown in the Supporting Information (Figs S2–3, Table S3–5). The list of specimens used and their provenance is given in Supplemental Appendix 1. We followed the systematic treatment of Wozencraft (2005). Only adult specimens were sampled; adults were recognized primarily by the

fully erupted permanent dentition and by the degree of epiphysial fusion of long bones. We defined a total of 124 linear measurements, 31 cranial and 93 postcranial (see below). This study required the sampling of variables in skeletons with all the unpaired postcranial elements (e.g. cervical vertebrae) and at least one bilateral element (e.g. femur) present, thus posing a serious challenge to finding such specimens in collections. Only 23 African specimens of a large sample examined (77 specimens, 30 with postcranial elements) in four major museums renowned for their holdings of felids met those requirements, highlighting the difficulty of generating a large data set for the postcranium of felids. Even if a greatly reduced measurement set was used (see below), the same completeness was still necessary to represent a reasonable amount of postcranial information. As one way to mitigate the effects of a reduced sample, a few Asian specimens of *F. chaus* (in supplemental material analyses), *Felis silvestris* Schreber 1777, *P. leo* and *P. pardus* (Linnaeus, 1758), as well as some specimens from zoos without visible anatomical alterations due to captivity, were added to the set of wild African specimens (see also statistical analyses below). Total number of specimens per species were as follows: *A. jubatus* (skull $n = 7$, postcranium $n = 4$), *C. caracal* (skull $n = 5$, postcranium $n = 2$), *F. chaus* (skull $n = 4$, postcranium $n = 4$), *F. margarita* (skull $n = 2$, postcranium $n = 2$), *F. nigripes* (skull $n = 3$, postcranium $n = 2$), *F. silvestris* (skull $n = 8$, postcranium $n = 3$), *L. serval* (skull $n = 5$, postcranium $n = 2$), *P. aurata* (skull $n = 3$, postcranium $n = 2$), *P. leo* (skull $n = 5$, postcranium $n = 3$), *P. pardus* (skull $n = 4$, postcranium $n = 2$).

Skull variables were taken from a previous study on Neotropical felids (Morales & Giannini, 2010). These variables were chosen to represent overall shape of skull components, as well as inferred trophic and sensory functions (see Fig. S1; Appendix S2 in the Supporting Information). The postcranial variables were selected to combine the description of form of each chosen element, and presumed function during locomotion and hunting (Figs 1–3). A commented definition of each postcranial variable is provided in the Appendix S3.

Statistical analysis

We performed Principal Component Analyses (PCA) based on the variance-covariance matrices of untransformed measurements to describe morphofunctional variation in three data sets: a) skull-only variables, hereafter 'skull data set'; b) postcranial-only variables, hereafter 'postcranial data set'; and c) skull + postcranial variables, hereafter 'combined data set'. Each analysis was performed with African specimens only, and including Asian specimens for those few species poorly represented by African specimens in the postcranial sample (see above). To explore species segregation in morphospace, we depicted species polygons (inclusive of all specimens of each species) on the ordination diagrams. Sexual dimorphism was not taken into account due to small sample size for multivariate testing. We performed an additional PCA analysis of the combined data set correcting for body size differences using the geometric mean to transform the original variables (e.g. Meachen-Samuels & Van Valkenburgh, 2009a). This analysis effectively removes pure-size effects present in raw measurements, although not morphological variation due to allometry. We performed additional analyses with a reduced set of postcranial and cranial variables (8 for skull and 19 for postcranial measurements) with the aim of testing the specimen sample-size effect by maximizing the specimen-to-variable ratio. Variables included in this analysis were for cranium: ATL, alveolar lower toothrow length; CBL, condylobasal length; CG, load arm of the C; FTL, *fossa temporalis* length; IOW, interorbital width; MeD, mandible depth; PC, post-orbital constriction and ZB, zigomatic breath; and for postcranium: A, length of the origin area of the *m. anconeus*; F, length of the femur; Fi, length of the fibula; GL, insertion of the *gastrocnemius caput laterale*; GM, insertion of the *gastrocnemius caput mediale*; H, total length of the humerus; HD, distal width of the humerus; IQ, length of the *corpus ossi ischii*; LDT, length of the deltoid tuberosity; LI, length of the ilium; MC, length of the *margo cranialis*; P, length of the pelvis; PQR, length of the insertion of the *m. pronator quadratus*; PR, length of the pectoral ridge; R, total length of the radius; T, length of the tibia; U, length of the ulna; WP, width of the pelvis at the ischiatic spine; WPI, width of the pelvis at the cranial border of the ilium (Figs 2 and 3, Fig. S1; see also Appendix S2 and S3 for details). This variable set represents the minimal set that covers the basic features of all considered relevant cranial structures and postcranial elements. The analyses included postcranial and combined data sets (corrected and not corrected by size) with and without *F. chaus*. Results including *F. chaus* are presented in Supporting Information (Fig. S4; Tables S9–11).

We used Canonical Phylogenetic Ordination (hereafter CPO; Giannini, 2003) to identify the fraction of morphological variation explained by historical factors (phylogenetic nestedness) in our data sets. This phylogenetic comparative method is a regression or ordination technique that uses linear constraints from an external, independent matrix composed by binary variables coding membership to clades – a tree matrix. We used the felid phylogenetic tree from Johnson *et al.* (2006), pruned to include only African felid species, to construct our tree matrix. Clade variables 1–6 were defined as shown in Fig. 4. These variables represent tree partitions as in an unrooted tree (phylogenetic network). In these analyses, tree partitions were first tested individually, evaluating significance with 4 999 Monte Carlo permutations. A forward stepwise

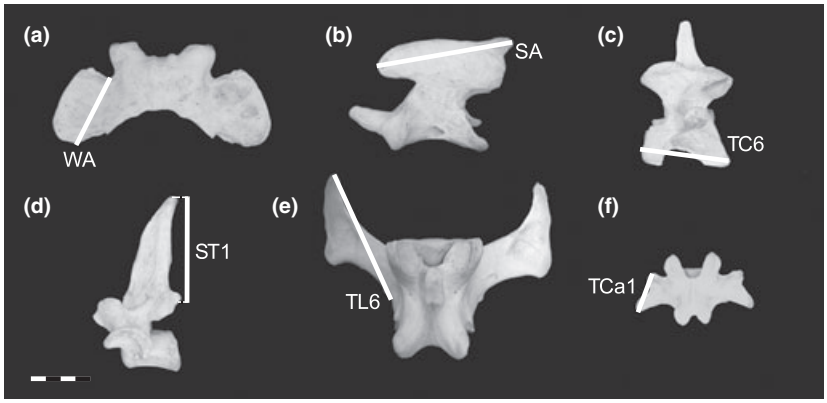

Fig. 1 Vertebral morphological variables measured in specimens of African felids represented on specimens of *Panthera leo*: a, b, c, d, f (AMNH 54 996); e (USNM 22 705). SA, length of the spinous process of the axis; ST1, high of the spinous process of the first thoracic vertebra; TC6, length of the transverse process of the sixth cervical vertebra; TCa1, length of the transverse process of the first caudal vertebra; TL6, length of the transverse process of the sixth lumbar vertebra; WA, length of the wing (= transverse process) of the atlas. For descriptions, see Appendix S3. Scale: bars = 10 mm. A high resolution version of this figure is available online in Appendix S4.

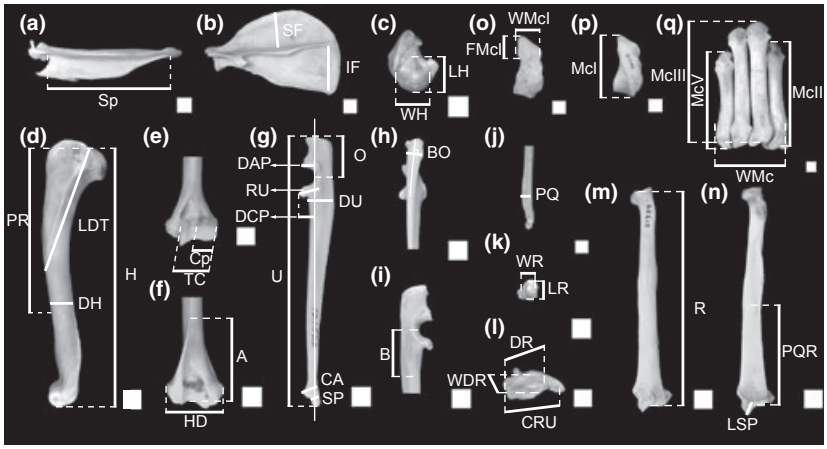

Fig. 2 Forelimb measurements represented on specimens of *Caracal caracal*: a (USNM 151 671-A49992), b, c, k (USNM 384 162); *Profelis aurata*: d, e, f, g, h, i (FMNH 121 528), j (USNM 278 523), n, m (AMNH 51 994); *Acinonyx jubatus*: l (USNM 163 098); and *Panthera leo*: o, p, q (AMNH 85 149). **a**, cranial view of the left scapula: Sp, length of the spine of the scapula. **b**, lateral view of the left scapula: IF, depth of the infraspinous fossa; SF, depth of the supraspinous fossa. **c**, proximal view of the left humerus: LH, length of the head of the humerus; WH, width of the head of the humerus. **d**, lateral view of the left humerus: DH, diameter of the humerus; H, total length of the humerus; LDT, length of the deltoid tuberosity; PR, length of the pectoral ridge. **e**, cranial view of the distal end of the left humerus: Cp, width of the capitulum; TC, width of the articular facet of the trochlea and capitulum. **f**, caudal view of the distal end of the left humerus: A, length of the origin area of the *m. anconeus*; HD, distal width of the humerus. **g**, lateral view of the left ulna: CA, depth of the process of the *circumferentia articularis*; DAP, depth of the anconeal process; DCP, depth of the medial coronoid process; DU, depth of the ulna; O, length of the olecranon; RU, length of the articular facet for the radius; SP, depth of the neck of the styloid process; U, total length of the ulna. **h**, caudal view of the proximal end of the ulna: BO, width of the caudal border of the olecranon. **i**, lateral view of the proximal end of the left ulna: B, insertion of the biceps. **j**, cranial view of the distal end of the left ulna: PQ, width at the ridge of insertion of the *m. pronator quadratus*. **k**, proximal view of the left radius: LR, length of the articular facet of the head of the radius; WR, width of the articular facet of the head of the radius. **l**, distal view of the left radius and humerus articulated: CRU, carpal width; DR, length of the articular facet of the distal end of the radius; WDR, width of the articular facet of the distal end of the radius. **m**, cranial view of the right radius: R, total length of the radius. **n**, caudal view of the left radius: LSP, length of the styloid process; PQR, length of the insertion of the *m. pronator quadratus*. **o**, palmar view of the left first metacarpal: FMcI, length of the medial articular facet of the distal end of the first metacarpal; WMcI, width of the first metacarpal. **p**, dorsal view of the left first metacarpal: McI, length of the first metacarpal. **q**, dorsal view of the articulated second to fifth metacarpals: McII, length of the second metacarpal; McIII, length of the third metacarpal; McV, length of the fifth metacarpal; WMc, width of the metacarpus. For further descriptions see Appendix S3. Scale: squares = 10 mm × 10 mm. A high resolution version of this figure is available online in Appendix S4.

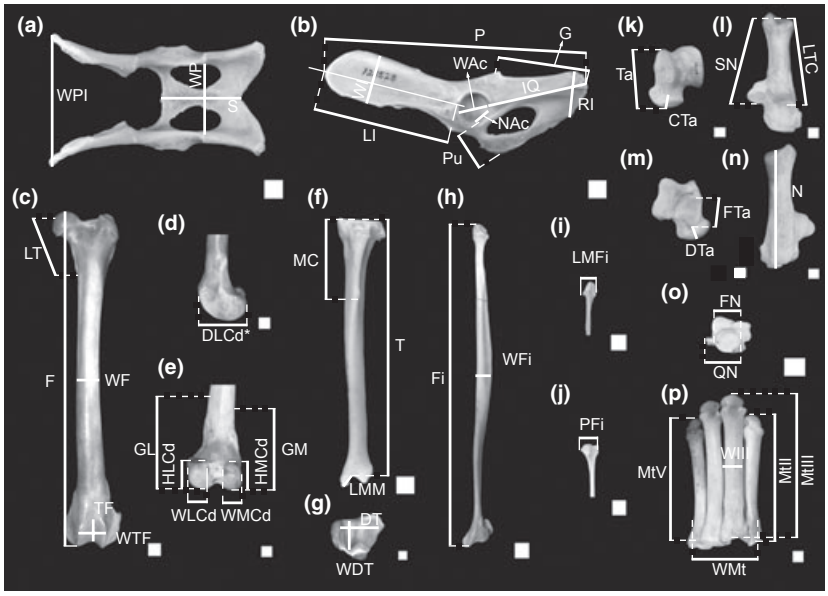

Fig. 3 Hindlimb measurements represented on specimens of *Profelis aurata*: a, b, f, i (FMNH 121 528), j, o (AMNH 51 994); *Acinonyx jubatus*: c, d (USNM 163 098), e (USNM 161 922); *Panthera leo*: g, k, l, m, n, p (AMNH 85 149); and *Panthera pardus*: h (USNM 254 536). **a**, dorsal view of the pelvis: S, length of the symphysis pelvis; WP, width of the pelvis at the ischiatic spine; WPI, width of the pelvis at the cranial border of the ilium. **b**, left lateral view of the pelvis; G, length of insertion of *m. gemelli*; IQ, length of the *corpus ossi ischii*; LI, length of the ilium; NAc, nonarticular area of the acetabular fossa; P, length of the pelvis; Pu, length of the pubis; RI, length of the *ramus ossi ischii*; WAc, width of the acetabular fossa; WI, width of the ilium. **c**, cranial view of the left femur: F, length of the femur; LT, position of the lesser trochanter; TF, length of the *trochlea femoris*; WF, width of the femur; WTF, width of the *trochlea femoris*. **d**, lateral view of the distal end of the left femur: DLCd, depth of the lateral condyle; * DMCd, depth of the medial condyle not shown. **e**, caudal view of the distal end of the left humerus: GL, insertion of the *gastrocnemius caput laterale*; GM, insertion of the *gastrocnemius caput mediale*; HLCd, height of the lateral condyle; HMCd, height of the medial condyle; WLCd, width of the lateral condyle; WMCd, width of the medial condyle. **f**, cranial view of the left tibia: LMM, length of the *malleolus medialis*; MC, length of the *margo cranialis*; T, length of the tibia. **g**, distal view of the tibia: DT, length of the distal articular facet; WDT, width of the distal articular facet. **h**, caudo-medial view of the left fibula: Fi, length of the fibula; WFi, maximum width of the fibula. **i**, caudal view of the proximal end of the right fibula: LMFi, latero-medial width of the proximal end of the fibula. **j**, lateral view of the proximal end of the left fibula: PFi, antero-posterior width of the proximal end of the fibula. **k**, dorsal view of the talus: CTa, length of the neck and head of the talus; Ta, length of the talus. **l**, dorsal view of the calcaneus: LTC, length of the *tuber calcanei*; SN, relative position of the sustentaculum. **m**, plantar view of the talus: DTa, nonarticular area in ventral view; FTa, length of the medial articular facet. **n**, plantar view of the calcaneus: N, length of the calcaneus. **o**, distal view of the calcaneus: FN, latero-medial width of the cubo-calcaneus articular facet; QN, distal width of the calcaneus. **p**, dorsal view of the articulated second to fifth metatarsals: MtII, length of the second metatarsal; MIII, length of the third metatarsal; MtV, length of the fifth metatarsal; WIII, width of the third metatarsal; WMt, width of the second to fifth metatarsals. For further descriptions see Appendix S3. Scale: squares = 10 mm × 10 mm. A high resolution version of this figure is available online in Appendix S4.

selection method was applied to all individually significant partitions (the so-called reduced tree matrix; see Giannini, 2003) to identify the combination of partitions that maximally explain morphological variance by common ancestry without redundancy. Significance was set to $\alpha = 0.01$, a compromise between typical $\alpha = 0.05$ and the Bonferroni-corrected value for increasing type I error due to multiple comparisons.

Results

Morphological patterns

Percentages of variation explained by morphology in each PCA axis did not vary substantially between analyses including or excluding Asian specimens; as a consequence, only results from all specimens are presented. The first PCA axis (PC1) in all analyses using raw data explained $\geq$ 95% of total variation (Table S1 and S6). All variables were positively correlated with PC1, indicating a size gradient in which four size groups could be recognized: the small-sized felids of the domestic cat lineage; the mid-sized felids of the caracal lineage; the medium-to-large *A. jubatus* and *P. pardus*, and the large *P. leo*.

Skull data set

The second principal component (PC2) explained 0.63% of total variation. On this axis, two variables, the post-orbital constriction (PC) and the length of

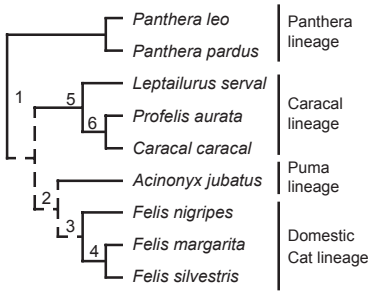

Fig. 4 Cladogram of African felid relationships based on Johnson *et al.* (2006). This tree is pruned to include only African species indicating groups used in canonical phylogenetic ordination.

the temporal fossa (FTL), presented high positive and negative loadings respectively (Fig. 5a, Fig. S1; Table S1). Other relatively less important variables on the PC2 were the zygomatic breath (ZB), the interorbital width (IOW; positive side of PC2) and the condylobasal length (CBL; negative side).

Postcranial data set

Distribution of species in this ordination diagram was roughly similar to the one obtained with the skull data set but with no interspecific overlap (Figs 5b and 6a). For both, complete and reduced postcranial data set, the PC2 explained 1.72% and 1.80% of morphological variation respectively (Table S1 and S6). Also in both analyses, the two most important variables positively correlated with scores along the PC2 were the length of origin of the *m. anconeus* (A) and the length of the insertion of the *m. pronator quadratus* (PQR; Tables S1 and S6). The former is an extensor and stabilizer of the elbow joint that also assists to *m. pronator quadratus* in forefeet pronation (Taylor & Weber, 1951; Gleason *et al.*, 1985; Evans, 1993; see also Appendix S3).

Measurements negatively correlated with PC2 were those describing the length of zeugopodial elements of both fore- and hindlimb (Fi, T, R, and U; Table S1); thus, long-legged felids lie towards the bottom of the PC1–PC2 plane (Figs 5b and 6a).

Combined data set

Raw data. In this nearly complete-skeleton analysis, PC2 explained the 2.65% and the 3.11% of total variance in full and reduced data sets respectively (Table S1 and S6). Measurements with higher positive scores on the PC2 were CBL, ZB and CG (the load arm of the canine), while the length of the fibula (Fi), tibia (T), radio (R) and ulna (U) were negatively related to it.

Size corrected. PC1 of analyses with complete and reduced data sets explained > 56% of total variation

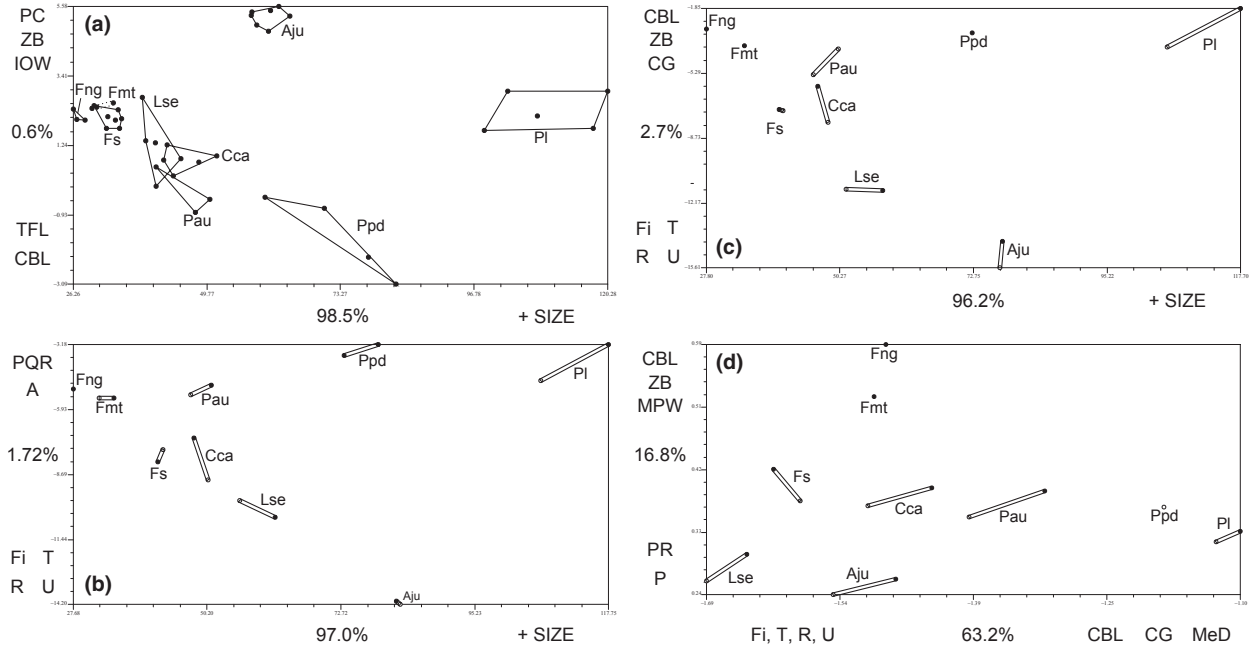

Fig. 5 Normalized ordination diagrams of principal components analyses (specimen scores scaled to unit eigenvector) performed for 9 species of African felids (all but *Felis chaus*) with the complete postcranial data set. **a**, Skull-only data set, note the graphic is mirrored to make it comparable to other diagrams in the Figure. **b**, Postcranium only data set. **c**, Combined data set. **d**, Combined data set, size corrected. Abbreviations: Aju, *Acinonyx jubatus*, Cca, *Caracal caracal*, Fmt, *Felis margarita*, Fng, *Felis nigripes*, Fs, *Felis silvestris*, Lse, *Leptailurus serval*, Pau, *Profelis aurata*, Pl, *Panthera leo*, Ppd, *Panthera pardus*.

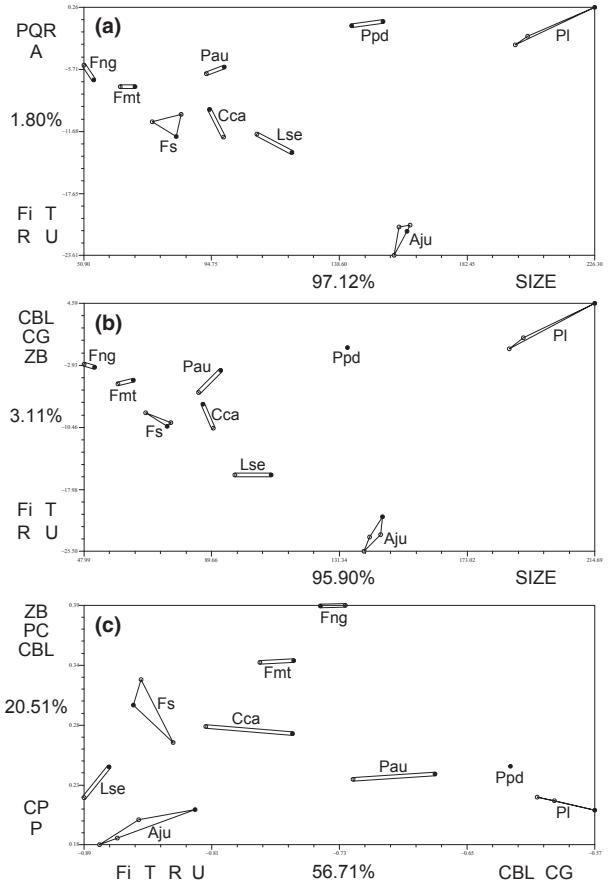

Fig. 6 Normalized ordination diagrams of principal components analyses (specimen scores scaled to unit eigenvector) performed for 9 species of African felids (all but *Felis chaus*) with the reduced postcranial data set. a, Postcranium-only data set. b, Combined data set. C, Combined data set, size corrected. Abbreviations: Aju, *Acinonyx jubatus*; Cca, *Caracal caracal*; Fmt, *Felis margarita*; Fng, *Felis nigripes*; Fs, *Felis silvestris*; Lse, *Leptailurus serval*; Pau, *Profelis aurata*; Pl, *Panthera leo* and Ppd, *Panthera pardus*.

(Figs 5d and 6c; Table S1 and S6). Using the complete postcranial data set, three cranial measurements (CBL; CG; and mental depth, MeD; Fig. S1) were the most important variables on the positive side of PC1, while in the reduced data set only the first two of these variables yielded high values. In the analyses of both data sets, the most important variables loading towards the negative side of PC1 were the length of the tibia (T) and fibula (Fi), followed by the length of the radio (R) and the ulna (U).

The PC2 of both data sets explained > 16% of total size-corrected variation. Three cranial measurements (CBL, ZB and mastoid processes width, MPW; Fig. S1; Table S1 and S6) were positively correlated with PC2, whereas the lengths of the pelvis (P) and the pectoral ridge (PR; Figs 2 and 3) were correlated negatively.

Phylogenetic patterns

All CPO analyses performed (with the complete postcranial data set when convenient) indicated a strong phylogenetic component to the morphological variation (Table 1). For the skull data set, four tree partitions individually explained a significant fraction of the total morphological variation (c. 20.6–69%; Table 1). Stepwise selection retained partitions 1, 3 and 2, in this order (with $P \leq 0.01$; Table S2). Altogether, these tree partitions explained 84.0% of total variation and represented the major lineages of African felids (Fig. 4). For the complete postcranium data set, analysis of individual tree partitions showed that partitions 1 and 3 were significant, individually explaining 40.8–53.5% of total morphological variation ($P \leq 0.01$; Table 1). Only partition 1 was retained by the stepwise model (with $P \leq 0.01$; Table S2), similarly capturing 53.5% of total variation. Probability associated to clade 3 ($P = 0.0\ 118$) was very close to alpha (= 0.01) explaining 16.7% of variance (Table S2). For the reduced postcranial data set only, individually significant groups were 1 and 3 (47.8–50.7%; $P \leq 0.01$; Table S7), and both were retained in the stepwise model ($P \leq 0.001$; Table S8). For the combined data set of complete postcranial variables with and without size correction, individual tests indicated that only partition 1 (pantherines vs. felines) was significant, explaining 59.2% and 31.4% of total variation respectively ($P \leq 0.01$, Table 1). In the combined data set with reduced set of postcranial variables not corrected by size, individually significant groups were only 1 and 3 (47.0–54.1%; $P \leq 0.001$; Table S7), and they both were retained at the stepwise model ($P \leq 0.001$; Table S8). Clades 1 and 2 significantly explained part of the morphological variation in the combined data set of the reduced set of postcranial variables (size-corrected; 17.4–19.7%; $P \leq 0.01$; Table S7), but only clade 1 was retained in the stepwise model ($P \leq 0.01$; Table S8).

Discussion

Morphological patterns

The different data sets showed distinct patterns of distribution of individuals and species in morphospace, which we interpret as follows.

Skull data set

Most important variables recovered by the PC2, postorbital constriction (PC) and length of the temporal fossa (FTL), together with the zygomatic breath (ZB), represented the amount of space available for accommodating the mass of the temporal muscle (*m. temporalis*). Therefore, variation along the PC2 depicted relative bite force differences as provided by the temporal muscle, segregating species of comparable size (i.e. with

Table1 Results of Canonical Phylogenetic Ordination (CPO). Individual tests for each clade in tree of Fig.4, for each of the four data sets analysed in this study, using complete postcranial data set when convenient.

	Skull			Postcranium			Combined			Combined size corrected		
Clade	% Variance	*F*-value	*P*	% Variance	*F*-value	*P*	% Variance	*F*-value	*P*	% Variance	*F*-value	*P*
1	68.8	88.205	0.0002*	53.5	17.247	0.0026*	59.2	19.130	0.0072*	31.4	5.964	0.0018*
2	20.6	10.395	0.0030*	15.4	2.732	0.1244	10.6	1.543	0.2394	10.9	1.586	0.1264
3	34.7	21.218	0.0002*	40.8	10.341	0.0066*	10.6	1.543	0.2500	10.9	1.586	0.1156
4	21.5	10.972	0.0020*	25.5	5.125	0.0284	17.5	2.764	0.0882	8.8	1.259	0.2044
5	6.3	2.691	0.1082	6.3	1.004	0.3404	9.6	1.388	0.2750	10.6	1.549	0.1246
6	2.1	0.876	0.3694	6.6	1.057	0.3286	8.0	1.138	0.3160	5.6	0.767	0.6042

*Statistically significant.

similar scores on the PC1), both sympatric (*A. jubatus* and *P. pardus*) and parapatric [*Caracal caracal* (Schreber, 1776) and *P. aurata* (Temminck, 1827); Fig. 5a; see also Christiansen & Wroe, 2007; Sakamoto *et al*., 2009]. Individuals with stronger relative bite force lied to the negative side of PC2. Altogether, the other variables recovered by the PC2 (ZB; IOW; CBL) represented variation in overall shape differences, with more rounded skulls towards the positive side of PC2 (Fig. 5a). This trade-off between rounded skull with small *m. temporalis* and *vice versa* was previously reported by, for example, Prevosti *et al.* (2010) and Sicuro & Oliveira (2010). Interestingly, *A. jubatus* shows the more rounded skull and the less developed *m. temporalis*, thus, skull of this species seems structured to allow for the enlarged nasals and turbinates required for breathing and cooling in relation to the hunting mode. This would reduce *m. temporalis* mass and the skull might become shorter to provide greater mechanical advantage.

Segregation of species in this morphospace was incomplete. Still, overlapping species of small to mid-sized felids segregated to some extent along ecological axes. These include 1. habitat preference (e.g. *F. margarita* Loche 1858, a sandy desert specialist vs. *F. silvestris*, which inhabits primarily savannas; Fig. 5a); 2. prey size (e.g. *L. serval* is a small prey specialist, vs. *C. caracal* and *P. aurata,* which are more generalist hunters; Meachen-Samuels & Van Valkenburgh, 2009a; see also Kiltie, 1984); and 3. geographical distribution (e.g. *P. aurata* vs. *C. caracal* and *L. serval*; Sunquist & Sunquist, 2009). A similar pattern of ecological segregation has been reported in African jackals (Van Valkenburgh & Wayne, 1994).

In general, patterns of skull morphology in African felids were similar to those reported for South American felids (Morales & Giannini, 2010) and for the family (Sicuro & Oliveira, 2010). Variation in masseteric complex shown in Sicuro & Oliveira (2010) was not recovered by our analyses given a different set of measurements.

Postcranial data set

The most salient result of the postcranial analysis was the complete segregation of all species of the African felid ensemble, although a larger sample may help detect marginally overlapping species (Figs 5b and 6a). Important variables recovered on the positive side of the PC2 (the length of origin of the *m. anconeus*, A; and the length of the insertion of the *m. pronator quadratus*, PQ) are associated to the extension and stabilization of the elbow joint and forefeet pronation (Taylor & Weber, 1951; Gleason *et al*., 1985; Evans, 1993; see also Appendix S3). Large force applied during pronation facilitates climbing behaviour and helps in bringing large prey down. *Leptailurus serval* and *A. jubatus* differed from other felids of comparable size in the poor development of postcranial variables associated to these functions (A, PQR; Tables S1 and S6), which likely reflects cursoriality: leg motion in terrestrial species tends to be restricted to the parasagittal plane, rather than favouring rotation and pronation, to gain stability while walking and running (Jenkins & Camazine, 1977; Taylor, 1989; Ewer, 1998; Argot, 2001; Andersson & Werdelin, 2003), also, the loss of supination means that such carnivores cannot use their forelimbs for grappling or manipulation of prey items, suggesting a trade-off between cursoriality and prey procurement strategies (Andersson & Werdelin, 2003). These species rarely climb trees and hunt differently. *Acinonyx jubatus* usually employs pulling with the dew claw to cause the prey to lose balance and fall, then suffocating it on the ground (Eaton, 1972, 1974). *Leptailurus serval* falls vertically on small-mammal prey such as rodents (Geertsema, 1985) pretty much as a fox does (Sunquist & Sunquist, 2009); canids are also known by their restricted supinatory ability (Andersson & Werdelin,

2003). In addition, elbow structure in this species may represent an adaptation to decrease energy expenditure (Andersson & Werdelin, 2003). In contrast, *P. leo* and *P. pardus* exhibited the highest positive scores along PC2 of the postcranial set. These felids are inferred to have a well developed *m. pronator quadratus*. *Panthera pardus* is a scansorial species able to hunt for prey larger than itself; it climbs trees carrying prey to protect it from competitors (Sunquist & Sunquist, 2009). *Panthera leo* does not climb as frequently or as high as the leopard, but this felid is a large-prey specialist (see Sunquist & Sunquist, 2009; and citations therein). For both actions, climbing and dragging large prey down, pronation and adduction are important (Gonyea, 1978; Evans, 1993), so the *mm. pronator quadratus* and *anconeus* are likely stronger in these species.

Length of zeugopodial elements of both fore- and hindlimb (forearm and crus) were also key in structuring the postcranial morphospace (Fi, T, R, and U; Table S1; Fig. 5b and 6a). Increase of effective limb length gained by zeugopodial elongation is an important adaptation for cursoriality and speed (Taylor, 1989; Alexander, 1993; Ewer, 1998), whereas longer hindlimbs relative to forelimbs are generally regarded as an adaptation for jumping (Howell, 1944 in Gonyea, 1976). Long-legged felids lie towards the negative side of the PC2 (Figs 5b and 6a); thus, *A. jubatus* segregated from felids of comparable size, specifically *P. pardus*, along this dimension in the postcranial morphospace. This sprinting species is the fastest terrestrial animal in a short dash; its legs may reach about the length typical for a bovid of its size (Alexander, 1993; Day & Jayne, 2007). Morphological adaptations for speed and enhanced performance while running have been thoroughly studied in *A. jubatus* (e.g. Hildebrand, 1959, 1961; Hildebrand & Hurley, 1985; Alexander, 1993; Sharp, 1997; Hudson *et al*., 2011a,b). Also, *L. serval* differs from its closer relative, *C. caracal* (and other felids) primarily on zeugopodial length (but see Day & Jayne, 2007), but in *L. serval* this is not related to sprinting. When hunting in tall grass, *L. serval* uses its high stance and big ears to find its preferred prey – small rodents; once the prey is located, *L. serval* pounces with all four feet off the ground falling vertically on the prey (Sunquist & Sunquist, 2009). *C. caracal* (and *F. chaus*; see Supporting Information) lies between the specialized *L. serval* and the more generalized *P. aurata*, possibly reflecting its known ability for jumping. Position of *F. silvestris* in this morphospace would suggest it is better equipped for jumping that the other small felids included in the analysis.

Combined data set

Raw data. The pattern of distribution and segregation of species seen in the postcranial set persisted in the combined morphospace of raw data for both, the complete and reduced postcranial data sets (Figs 5c and 6b). This indicates a relatively stronger contribution of postcranium to the morphofunctional structuring of the African felid ensemble as compared with the skull data.

In this analysis, the fundamental variation represented in the PC2 revealed a gradient of morphotypes from short-legged felids with large and powerful skulls and stronger bite force, to long-legged felids with relative smaller, weaker skulls (Figs 5c and 6b; Table S1 and S6; for other results see below).

Size corrected. Segregation among species in the size-corrected morphospace with complete and reduced postcranial data set was also complete, although distribution of species was slightly different as compared with the results not corrected by size (Figs 5d and 6c; Table S1 and S6).

On the PC1 of the analysis of the complete postcranial data set, a longer load arm of the canine may seem unfavourable for the species bearing this feature; however, given that longer skulls corresponded to larger species, strength gained by greater temporal muscles may easily compensate for mechanical disadvantage of load arm in these species. This compensation likely was reflected also in the deeper mandible (high MeD) of large species, representing a strengthening of the area of the lower canine to endure greater force.

The length of the pelvis (P) was recovered as negatively correlated with the PC2. This measurement as a whole can be interpreted as composed of two parts, the length of the ilium (LI) and the length of the body of the ischium (IQ). IQ is the pelvic measurement that contributes the most to the extension of the pelvis (Table S1 and S6). Principal muscles related functionally to this part of the pelvis are *biceps femoris*, *semitendinosus* and *semimembranosus*; these muscles assist in thigh and tarsal extension and shank flexion (Taylor & Weber, 1951; Evans, 1993). In turn, the length of the ilium (LI) remained proportionally constant among the studied felids (Table S1 and S6).

Leptailurus serval and *A. jubatus* are remarkable for their high values of PR length. Development of the PR is usually related to holding strength during climbing [e.g. in guenons (Gebo & Sargis, 1994) and viverrids (Taylor, 1974)] and for grabbing large prey, although this is not always the case (e.g. in climbing tupaiids and marsupials; Szalay & Sargis, 2001; Sargis, 2002). In this case, we consider that longer pectoral insertions would help stabilizing parasagittal movements in long-legged felids (see Appendix S3 for more details). Although not among the highest loadings, it is interesting to note the inverse relationship present between autopod length and width; that is, wide and short in the positive side of the PC1, and long and narrow on the negative side. This pattern likely reflects cursoriality in the negative side and wider and stronger autopods in *P. leo* and *P. pardus*. Wider forefeet were found to be related to grabbing prey and other objects, for example, tree trunks

when climbing (Schmieder, 2000; Argot, 2001). The same can be extrapolated to hind feet, especially for *P. leo*, that uses them to stand on the ground while grabbing large prey with its forefeet; thus, wider feet provide efficient support on the ground.

When correcting by size in the complete data set, additional patterns of osteological variation were apparent (Fig. 5d). Three groups of felids could be recognized: small terrestrial species towards the top of the PC1–PC2 plane, long-legged terrestrial felids towards the bottom, and scansorial or consumers of large prey towards the centre of the morphospace. Hence, scansorial species have intermediate values of PC2 (i.e. in degree of elongation of the ischium and of the insertion of the pectoral muscles) and appeared positioned in-between small felids and the highly specialized *A. jubatus* and *L. serval*. Small felids may dispense from possessing these specialized anatomical features simply due to their small size. Among large-prey hunters, *P. leo* is characterized by preserving the aspect of a forest felid while inhabiting open areas (Gonyea, 1976). In our complete postcranial, size-corrected analysis, *P. leo* was only slightly displaced towards the more terrestrial species (Fig. 5d). This is in line with the idea that hunting large prey likely poses a strong constraint that keeps *P. leo*'s bodily proportions (Gonyea, 1976). This pattern seems to be unclear in the reduced data set (Fig.6c); as many variables were killed to improve the specimen-variable ratio (see McGarigal *et al.*, 2000), this in fact may reflect lack of morphological information such as autopodial differences.

An inverse relationship between overall head size and leg length emerges in skull + postcranium analysis, corrected or not by size. The lightly built, long-legged (Fi, T, R, U), small-headed (CBL, ZB, CG) *A. jubatus* and *L. serval* contrast with more ordinarily constructed felids of comparable size, *P. pardus* and *Caracal caracal* respectively. Small head likely represents one facet of reducing mass in felids with strenuous activities like frequent jumping and high-speed running (Taylor *et al.*, 1974; Hildebrand & Hurley, 1985). This requirement (mass reduction) in turn may constrain hunting mode and prey selection (Hayward *et al.*, 2006). Despite the recognized homogeneity in body plan of felids, and the direct competition prevailing among many species (e.g. *P. leo*, *P. pardus* and *A. jubatus*; Stuart & Wilson, 1988; Sunquist & Sunquist, 2002), our work afforded evidence of morphological variation that correlates with ecological niche segregation (see also Gonyea, 1976, 1978).

Phylogenetic patterns and the assembly of the African felid ensemble

Morphological variation may reflect historical events (e.g. Van Valkenburgh & Wayne, 1994). In the spirit of CPO (see Giannini, 2003), variation explained by phylogeny means in our study that morphology co-varied with cladogenesis to a large extent; thus, history of the African felid ensemble can be reconstructed from combining patterns of occupancy in morphospace with the sequence of cladogenetic events and arrival dates of ancestors of present-day lineages [from Johnson *et al.* (2006): molecular data; Werdelin & Lewis (2005); Peigné *et al.* (2008); Werdelin & Peigné (2010) and Werdelin *et al.* (2010): fossil data]. The following analysis mimics that of Morales & Giannini (2010) for Neotropical felids.

According to the fossil record, the first felids to arrive into Africa belonged to the domestic cat lineage about 7 Myr (Peigné *et al.*, 2008; Werdelin & Peigné, 2010). At present, three extant small felids belong to this lineage, of which *F. silvestris* and *F. margarita* overlap in skull morphology, segregating in habitat preference and habits. Also, *F. silvestris* may have been a latecomer, possibly not evolving in the continent. According to molecular dating, ancestors of the caracal lineage arrived in Africa at 8.5–5.6 Myr (Johnson *et al.*, 2006), although the first fossil records of *C. caracal* and *L. serval* in Africa are more recent, about 3.8–3.5 Myr (Middle Pliocene; Werdelin & Lewis, 2005), or possibly as old as 6 Myr (Werdelin & Peigné, 2010). This lineage diversified within the continent leaving three extant descendants, all mid-sized species which partially overlap in skull morphology but segregate in postcranial morphology and also ecologically and geographically. Each of these lineages established in mutually exclusive areas of the morphospace. When including *F. chaus*, a marginal overlap exists in skull morphology among these two lineages (see Supporting Information). Molecular estimates suggests that during early or middle Pliocene, *A. jubatus* (member of the Puma lineage) arrived to Africa, and later on species of *Panthera* entered the continent by the middle Pliocene (Johnson *et al.*, 2006). On the other hand, first fossil records for both these lineages are found in Africa at ca. 4 Myr (Werdelin & Peigné, 2010). All these forms that successively arrived to the continent occupied vacant areas of the morphospace, as predicted from analyses in the Neotropical felid ensemble (Morales & Giannini, 2010).

Conclusions

In spite of the morphological homogeneity attributed to felids in general, and limitations from material held at museums, we were able to detect significant morphofunctional and historical structuring among African felids that may help explain the coexistence of these strongly antagonistic species in the continent. Several morphofunctional factors segregated felid species in morphospace, including body size, bite force, length of the zeugopods, and origin or insertion of muscles related to pronation of the hand, extension of the thigh and stability in parasagittal-plane movements of the legs. Altogether, this interspecific variation imposes

a functional imprint on the relationships among species in morphospace. A general pattern of bodily proportions with functional significance was recovered; specifically, the opposition of lightly built, long-legged terrestrial felids with small heads and weak bite forces vs. large-prey hunters and scansorial species with shorter, stronger legs and larger skulls with more powerful bite force. In addition, more subtle variation in degree of development of the length of the pectoral ridge and elongation of the ischium can be recognized to identify three groups, namely small felids, highly cursorial *A. jubatus* and *L. serval*, and scansorial species together with large-prey hunters. Species within each of the last two groups differed from each other along a gradient of body size. In historical perspective, the African felid ensemble likely was assembled by the successive addition of ancestors of distinct felid lineages that occupied vacant areas of morphospace and speciated in Africa throughout the Pliocene-to-Recent history of the continent.

Acknowledgments

We thank Don E. Wilson, Kristofer M. Helgen, Alfred L. Gardner, Linda Gordon, Jeremy Jacobs (National Museum of Natural History, Washington, DC), Lawrence Heaney, William Stanley (Field Museum of Natural History, Chicago), Nancy Simmons, Darrin Lunde, Eileen Westwig (American Museum of Natural History, New York), and David Flores and Valentina Segura (Museo Argentino de Ciencias Naturales 'Bernardino Rivadavia', Buenos Aires) for access to the specimens under their care. We also thank Lars Werdelin, Kristofer Helgen and Francisco Prevosti for greatly improving this manuscript with their comments and suggestions. Thanks to Christine Argot and María Sandoval for early comments and references and Juan Pablo Sidán for picture editing. M.M. Morales thanks the National Museum of Natural History, Smithsonian Institution, Washington D.C. for a Short Term Visitor Fellowship (special thanks to Don E. Wilson and Kristofer M. Helgen). We thank CONICET and PICT-2008-1798 (Argentina).

References

Alexander, R.M. 1993. Legs and locomotion of Carnivora. In: *Mammals as Predators* (N. Dunstone & M.L. Gormaneds), Symposia of the Zoological Society of London **65**: 1–13. Clarendon Press, Oxford, New York.

Andersson, K. & Werdelin, L. 2003. The evolution of cursorial carnivores in the Tertiary: implications of elbow joint morphology. *P. Roy. Soc. B-Biol. Sci.* **270**: S163–S165.

Archibold, O.W. 1995. *Ecology of World Vegetation*. Chapman and Hall, London.

Argot, C. 2001. Functional-adaptative anatomy of the forelimb in the Didelphidae, and paleobiology of the Paleocene Marsupials *Mayulestes ferox* and *Pucadelphys andinus*. *J. Morphol.* **247**: 51–79.

Chinchilla, F. 1997. La dieta del jaguar (*Panthera onca*), el puma (*Felis concolor*), y el manigordo (*Felis pardalis*)(Carnivora: Felidae) en el Parque Nacional Corcovado, Costa Rica. *Rev. Bio. Trop.* **45**: 1223–1229.

Christiansen, P. 2008. Evolution of skull and mandible shape in cats (Carnivora: Felidae). *PLoS ONE* **3**: e2807.

Christiansen, P. & Wroe, S. 2007. Bite forces and evolutionary adaptations to feeding ecology in carnivores. *Ecology* **88**: 347–358.

Day, L.M. & Jayne, B.C. 2007. Interspecific scaling of the morphology and posture of the limbs during the locomotion of cats (Felidae). *J. Exp. Biol.* **210**: 642–654.

Dayan, T., Simberloff, D., Tchernov, E. & Yom-Tov, Y. 1990. Feline canines: community-wide character displacement among the small cats of Israel. *Am. Nat.* **136**: 39–60.

Eaton, R.L. 1972. An experimental study of predatory and feeding behavior in the cheetah. *Z. Tierpsychol.* **31**: 270–80.

Eaton, R.L. 1974. Predatory and killing behavior. In: *The Cheetah - The Biology, Ecology, and Behavior of an Endangered Species* (R.L. Eaton, ed), pp. 129–553. Van Nostrand Reinhold Company, New York.

Emmons, L.H. 1987. Comparative feeding ecology of felids in a Neotropical rainforest. *Behav. Ecol. Sociobiol.* **20**: 271–283.

Evans, H.E. 1993. *Miller's Anatomy of the Dog*, 3rd edn. WB Saunders Company, Philadelphia.

Ewer, R.F. 1998. *The Carnivores*. Cornell University Press, New York.

Fryxell, J.M., Mosser, A., Sinclair, A.R.E. & Packer, C. 2007. Group formation stabilizes predator-prey dynamics. *Nature* **449**: 1041–1044.

Gebo, D.L. & Sargis, E.J. 1994. Terrestrial adaptations in the postcranial skeletons of guenons. *Am. J. Phys. Anthropol.* **93**: 341–371.

Geertsema, A.A. 1985. Aspects of the Ecology of the serval *Leptailurus serval* in the Ngorongoro crater. *Tanzania. Neth. J. Zool.* **35**: 527–610.

Giannini, N.P. 2003. Canonical phylogenetic ordination. *Syst. Biol.* **52**: 684–695.

Gleason, T.F., Goldstein, W.M. & Ray, R.D. 1985. The function of the anconeus muscle. *Clin. Orthop. Relat. R.* **192**: 147–148.

Gonyea, W.J. 1976. Adaptive differences in the body proportions of large felids. *Acta Anat.* **96**: 81–96.

Gonyea, W.J. 1978. Functional implications of forelimb anatomy. *Acta Anat.* **102**: 111–121.

Haas, S.K., Hayssen, V. & Krausman, P.R. 2005. Mammalian species - *Panthera leo*. *Mamm. Species* **762**: 1–11.

Hayward, M.W., Hofmeyr, M., O'Brien, J. & Kerley, G.I.H. 2006. Prey preferences of the cheetah (*Acinonyx jubatus*) (Felidae: Carnivora): morphological limitations or the need to capture rapidly consumable prey before kleptoparasites arrive? *J. Zool.* **270**: 615–627.

Hildebrand, M. 1959. Motions of the running cheetah and horse. *J. Mammal.* **40**: 481–495.

Hildebrand, M. 1961. Further studies on locomotion of the cheetah. *J. Mammal.* **42**: 84–91.

Hildebrand, M. & Hurley, J.P. 1985. Energy of the oscillating legs of a fast-moving cheetah, pronghorn, jackrabbit and elephant. *J. Morphol.* **184**: 23–31.

Huang, G.T., Rosowski, J.J., Ravicz, M.E. & Peake, W.T. 2002. Mammalian ear specializations in arid habitats: structural and functional evidence from sand cat (*Felis margarita*). *J. Comp. Physiol. A.* **188**: 663–681.

Hudson, P.E., Corr, S.A., Payne-Davis, R.C., Clancy, S.N., Lane, E. & Wilson, A.M. 2011a. Functional anatomy of the cheetah (*Acinonyx jubatus*) hindlimb. *J. Anat.* **218**: 363–374.

Hudson, P.E., Corr, S.A., Payne-Davis, R.C., Clancy, S.N., Lane, E. & Wilson, A.M. 2011b. Functional anatomy of the cheetah (*Acinonyx jubatus*) forelimb. *J. Anat.* **218**: 375–385.

Hutchinson, G.E. 1957. Concluding remarks. *Cold Spring Harb. Symp. Quant. Biol.* **22**: 415–427.

Jenkins, F.A. & Camazine, S.M. 1977. Hip structure and locomotion in ambulatory and cursorial carnivores. *J. Zool.* **181**: 351–370.

Johnson, W.E., Eizirik, E., Pecon-Slattery, J., Murphy, W.J., Antunes, A., Teeling, E. *et al.* 2006. The late Miocene radiation of modern Felidae: a genetic assessment. *Science* **311**: 73–77.

Kiltie, R.A. 1984. Size ratios among sympatric Neotropical cats. *Oecologia* **61**: 411–416.

Kiltie, R.A. 1988. Interspecific size regularities in tropical felids assemblages. *Oecologia* **76**: 97–105.

Kitchener, A. 1991. *The Natural History of the Wild Cats*. Cornell University Press, Ithaca, New York.

Konecny, M.J. 1989. Movement patterns and food habits of four sympatric carnivore species in Belize, Central America. *Adv. Neotrop. Mamm.* **1989**: 243–264.

McGarigal, K., Cushman, S.A. & Stafford, S.G. 2000 *Multivariate Statistics for Wildlife and Ecology Research*. Springer-Verlag, New York.

Meachen-Samuels, J. & Van Valkenburgh, B. 2009a. Craniodental indicators of prey size preference in the Felidae. *Biol. J. Linn. Soc.* **96**: 784–799.

Meachen-Samuels, J. & Van Valkenburgh, B. 2009b. Forelimb indicators of prey-size preference in the felidae. *J. Morphol.* **270**: 729–744.

Morales, M. & Giannini, N.P. 2010. Morphofunctional patterns in Neotropical felids: species coexistence and historical assembly. *Biol. J. Linn. Soc.* **100**: 711–724.

Peigné, S., Debonis, L., Mackaye, H., Likius, A., Vignaud, P. & Brunet, M. 2008. Late Miocene Carnivora from Chad: Herpestidae, Viverridae and small-sized Felidae. *C. R. Palevol.* **7**: 499–527.

Prevosti, F.J., Turazzini, G.F. & Chemisquy, M.A. 2010. Morfología craneana en tigres dientes de sable: alometría, función y filogenia. *Ameghiniana* **47**: 239–256.

Ranta, E. & Kaitala, V. 2005. *A leap for lion populations. Science* **307**: 365–366.

Sakamoto, M., Lloyd, G.T. & Benton, M.J. 2009. Phylogenetically structured variance in felid bite force: the role of phylogeny in the evolution of biting performance. *J. Evolution. Biol.* **23**: 463–478.

Sargis, E. 2002. Functional morphology of the forelimb of tupaiids (Mammalia, Scandentia) and its phylogenetic implications. *J. Morphol.* **253**: 10–42.

Schmieder, J-U. 2000. Killing behavior in *Smilodon fatalis* (Mammalia, Carnivora, Felidae) based on functional anatomy and body proportions of the front- and hind limbs. Thesis. Geologisches Institut der Eberhardt-Karls-Universität Tübingen.

Sharp, N.C.C. 1997. Timed running speed of a cheetah (*Acinonyx jubatus*). *J. Zool.* **241**: 493–494.

Sicuro, F.L. 2011. Evolutionary trends on extant cat skull morphology (Carnivora: Felidae): a three-dimensional geometrical approach. *Biol. J. Linn. Soc.* **103**: 176–190.

Sicuro, F.L. & Oliveira, L.F.B. 2010. Skull morphology and functionality of extant Felidae (Mammalia: Carnivora): a phylogenetic and evolutionary perspective. *Zool. J. Linn. Soc.* **161**: 414–462.

Skinner, J.D. 1979. Feeding behaviour in Caracal *Felis caracal*. *J. Zool.* **189**: 523–525.

Skinner, J.D. & Smithers, R.H.N. 1990 *The Mammals of the Southern African Subregion*. University of Pretoria, South Africa.

Spoor, C.F. & Badoux, D.M. 1988. Descriptive and functional myology of the back and hindlimb of the Striped Hyena (*Hyaena hyaena*, L. 1758). *Anat. Anzeiger* **167**: 313–321.

Stuart, C.T. & Wilson, V.J. 1988. *The Cats of Southern Africa*. A summary of the current knowledge of the seven cat species occurring in the southern Africa, with emphasis on conservation and status. IUCN/SSC Cat Specialist Group African Carnivore Survey and Chipangali Wildlife Trust. The Chipangali wildlife trust, Bulawayo, Zimbabwe.

Sunquist, M.E. & Sunquist, F.C. 2002 *Wild Cats of the World*. University of Chicago Press, Chicago.

Sunquist, M.E. & Sunquist, F.C. 2009. Family Felidae. In: *Handbook of Mammals of the world, Vol. 1. Carnivores* (D.E. Wilson & R.A. Mittermeir, eds.), pp. 54–168. Lynx editions, Barcelona.

Szalay, F.S. & Sargis, E.J. 2001. Model-based analysis of postcranial osteology of marsupials from the Palaeocene of Itaboraí (Brazil) and the phylogenetics and biogeography of Metatheria. *Geodiversitas* **23**: 139–302.

Taylor, M.E. 1974. The functional anatomy of the forelimb of some African Viverridae (Carnivora). *J. Morphol.* **143**: 307–336.

Taylor, M.E. 1989 Locomotor adaptations by Carnivores. In: *Carnivore Behavior, Ecology and Evolution* (J.L. Gittleman, ed), pp. 382–409. Cornell University Press, Ithaca, New York.

Taylor, W.T. & Weber, R.J. 1951 *Functional Mammalian Anatomy (with special reference to the Cat)*. D Van Nostrand Company, Princeton, New Jersey, New York.

Taylor, C.R., Shkolnik, A., Dmiél, R., Baharav, D. & Borut, A. 1974. Running in cheetahs, gazelles, and goats: energy cost and limb configuration. *Am. J. Physiol.* **227**: 848–850.

Tyabji, H.N. 1990. A hunting technique of the jungle cat *Felis chaus*. *J. Bombay Nat. Hist. Soc.* **87**: 134.

Van Valkenburgh, B. & Wayne, R.K. 1994. Shape divergence associated with size convergence in sympatric East African jackals. *Ecology* **75**: 1567–1581.

Werdelin, L. 1983. Morphological patterns in the skulls of cats. *Biol. J. Linn. Soc.* **19**: 375–391.

Werdelin, L. 2012. A new genus and species of Felidae (Mammalia) from Rusinga Island, Kenya, with notes on early Felidae of Africa. *Estud. Geol.* **67**: 217–222.

Werdelin, L. & Lewis, M.E. 2005. Plio-Pleistocene Carnivora of eastern Africa: species richness and turnover patterns. *Zool. J. Linn. Soc.* **144**: 121–44.

Werdelin, L. & Peigné, S. 2010. Carnivora. In: *Cenozoic Mammals of Africa* (L. Werdelin, W.J. Sanders, eds), pp. 609–663. University of California Press, Berkeley.

Werdelin, L., Yamaguchi, N., Johnson, W.E. & O'Brien, S.J. 2010. Phylogeny and evolution of cats (Felidae). In: *Biology and Conservation of Wild Felids* (D.W. Macdonald, A.J. Loveridge, eds), pp. 59–88. Oxford University Press, Oxford.

Wozencraft, W.C. 2005. Order Carnivora, Family Felidae. In: *Mammals Species of the World: a Taxonomic and Geographic Reference*, Vol. 1, 3rd edn (D.E. Wilson & D.M. Reeder, eds), pp. 532–545. The Johns Hopkins University Press, Baltimore.

Supporting information

Additional Supporting Information may be found in the online version of this article:

Figure S1 Skull variables used in this study.

Figure S2 PCA ordination diagrams using the complete postcranial data set with *Felis chaus*.

Figure S3 Cladogram with groups used in CPO analysis with *Felis chaus*.

Figure S4 PCA ordination diagrams using reduced postcranial data set with *Felis chaus*.

Table S1 PCA results for the skull, postcranial, combined data set and combined data set size corrected using complete postcranial data set without *Felis chaus*.

Table S2 Canonical Phylogenetic Ordination results for stepwise selection method using complete postcranial data set without *Felis chaus*.

Table S3 PCA results for the skull, postcranial, combined data set and combined data set size corrected using complete postcranial data set with *Felis chaus*.

Table S4 CPO results for individual tests using complete postcranial data set with *Felis chaus*.

Table S5 CPO results for stepwise selection method using complete postcranial data set with *Felis chaus*.

Table S6 PCA results for the postcranial and combined data set corrected and not corrected by size using the reduced postcranial data set without *Felis chaus*.

Table S7 CPO results for individual tests using the reduced postcranial data set without *Felis chaus*.

Table S8 CPO results for stepwise selection method using the reduced postcranial data set without *Felis chaus*.

Table S9 PCA results for the postcranial and combined data sets corrected and not corrected by size using the reduced postcranial data set with *Felis chaus*.

Table S10 CPO results for individual tests using the reduced postcranial data set with *Felis chaus*.

Table S11 CPO results for stepwise selection method using the reduced postcranial data set with *Felis chaus*.

Appendix S1 Specimens examined.

Appendix S2 List and description of cranial measurements.

Appendix S3 List and description of postcranial measurements.

Appendix S4 High resolution version of Figs 1–3.

Received 29 September 2012; revised 27 November 2012; accepted 17 December 2012